A Green Approach to the Synthesis of Graphene Nanosheets

Hui-Lin Guo,[†,‡] Xian-Fei Wang,[†] Qing-Yun Qian,[†] Feng-Bin Wang,[†] and Xing-Hua Xia[†,*]

[†]Key Laboratory of Analytical Chemistry for Life Science, School of Chemistry and Chemical Engineering, Nanjing University, Nanjing 210093, China, and [‡]Key Laboratory of Synthetic and Natural Functional Molecule Chemistry, College of Chemistry and Materials Science, Northwest University, Xi'an 710069, China

ABSTRACT Graphene can be viewed as an individual atomic plane extracted from graphite, as unrolled single-walled carbon nanotube or as an extended flat fullerene molecule. In this paper, a facile approach to the synthesis of high quality graphene nanosheets in large scale through electrochemical reduction of exfoliated graphite oxide precursor at cathodic potentials (completely reduced potential: −1.5 V) is reported. This method is green and fast, and will not result in contamination of the reduced material. The electrochemically reduced graphene nanosheets have been carefully characterized by spectroscopic and electrochemical techniques in comparison to the chemically reduced graphene-based product. Particularly, FTIR spectra indicate that a variety of the oxygen-containing functional groups have been thoroughly removed from the graphite oxide plane *via* electrochemical reduction. The chemically converted materials are not expected to exhibit graphene's electronic properties because of residual defects. Indeed, the high quality graphene accelerates the electron transfer rate in dopamine electrochemistry (ΔE_p is as small as 44 mV which is much smaller than that on a glassy carbon electrode). This approach opens up the possibility for assembling graphene biocomposites for electrocatalysis and the construction of biosensors.

KEYWORDS: graphene nanosheets · electrochemical synthesis · electrocatalysis · FTIR · dopamine

Graphene nanosheet is a one-atom-thick planar sheet of sp^2-bonded carbon atoms, which are densely packed in a honeycomb crystal lattice, attracting tremendous attention from both fundamental research (where it forms a new, unexpected bridge between condensed matter and quantum field theory) and possible applications.[1] This unique nanostructure holds great promise for potential applications in many technological fields such as nanoelectronics,[2,3] sensors,[4,5] nanocomposites,[6,7] batteries,[8] supercapacitors, and hydrogen storage.[9] In this context, the preparation of high-quality 2D graphene sheets is the first and most crucial step, as the existence of residual defects will heavily impact the electronic properties of graphene. Mechanical cleavage of graphite originally led to the discovery of graphene sheets;[9,10] however, the low productivity of this method makes it unsuitable for large-scale utilization. Later, ultrathin epitaxial graphene sheets were grown on a single-crystal silicon carbide by vacuum graphitization. This approach allows the fabrication of a patterned graphene structure, which is desirable for electronic applications.[11−13] Furthermore, graphene sheets can be made from rapidly thermal expanded graphite, but it hardly results in complete exfoliation of graphite to the atomic level of individual graphene sheets.[14−17] Recently, chemical reduction of exfoliated graphite oxide (GO), a soft chemical synthesis route using graphite as the initial material was reported.[18−22] All these are efficient approaches to bulk production of graphene-based sheets at low cost. Stankovich *et al.*[18,19] and Wang *et al.*[21] carried out the chemical reduction of exfoliated graphene oxide sheets with hydrazine hydrate and hydroquinone as the reducing agents, respectively. Kamat *et al.* proposed photocatalytic reduction of graphite oxide.[22] However, the excessive reducing agents employed in this approach could contaminate the resulting materials, and, on the other hand, oxygenated species that cannot so far be fully removed by chemical treatment degrade the electronic properties of the product and further limit the application.[23]

Electrochemical method is an effective tool to modify electronic states *via* adjusting the external power source to change the Fermi energy level of electrode materials surface. For the first time, we report a facile and fast approach to the synthesis of high quality graphene nanosheets in large scale by electrochemical reduction of the exfoliated GO at a graphite electrode, and the reaction rate can be accelerated by increasing the reduction temperature. Defects will be further eliminated in this way

*Address correspondence to xhxia@nju.edu.cn.

Received for review March 3, 2009 and accepted August 13, 2009.

Published online August 19, 2009.
10.1021/nn900227d CCC: $40.75

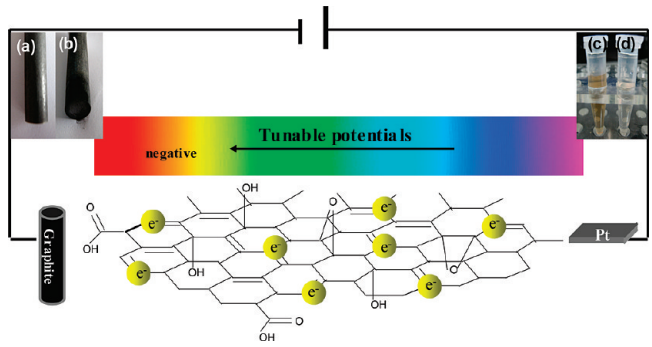

Figure 1. Experimental setup illustration and the optical images of the graphite electrode and the GO suspension before (a,c) and after (b,d) electrochemical reduction. The electrochemical reduction potential of the exfoliated GO dispersion at a graphite electrode was −1.5 V *vs* SCE.

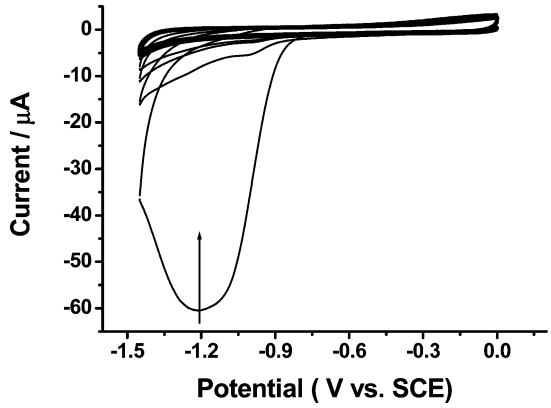

Figure 2. Cyclic voltammograms of a GO-modified GCE in PBS (pH 5.0) saturated with nitrogen gas at a scan rate of 50 mV/s. The potential started at 0.0 V.

or by annealing. This method has three clear advantages: it is new, fast, and green, no toxic solvents are used and therefore will not result in contamination of the product; the high negative potential can overcome the energy barriers for the reduction of oxygen functionalities (−OH, C−O−C on the plane and −COOH on the edge), thus, the exfoliated GO can be efficiently reduced; the modified electrode can be further used in bioanalysis, biosensor, and electrocatalysis. Finally, we report the electrocatalytic reaction of dopamine accelerated by graphene.

RESULTS AND DISCUSSION

We use exfoliated graphite oxide prepared by oxidizing graphite flakes in acidic medium as the starting material for the preparation of graphene according to the modified method of Hummer.[24,25] A wide range of oxygen groups bonded onto the surface of GO increases the charged capacity, thereby, increasing the dispersion of GO in water to a greater extent. Electrochemical reduction of the exfoliated GO was performed on a graphite working electrode at different cathodic potential in a GO dispersion with magnetic stirring. The electrochemical setup as well as the optical images of the graphite electrode and the GO suspension before and after electrochemical reduction is illustrated in Figure 1.

The cyclic voltammograms (Figure 2) of a GO-modified glassy carbon electrode (GCE) in a potential range from 0.0 to −1.5 V shows a large cathodic current peak at −1.2 V with a starting potential of −0.75 V. This large reduction current should be due to the reduction of the surface oxygen groups since the reduction of water to hydrogen occurs at more negative potentials (*e.g.*, −1.5 V). In the second cycle, the reduction current at negative potentials decreases considerably and disappears after several potential scans. This demonstrates that the reduction of surface-oxygenated species at GO occurs quickly and irreversibly and the exfoliated GO could be reduced electrochemically at negative potentials.

Differential pulse voltammetries (DPVs) and cyclic voltammograms (CVs) were measured to examine the time required for electrochemical reduction of exfoliated GO at −1.3 V (*vs* SCE) in 10 mmol/L pH5.0 PBS (K_2HPO_4/KH_2PO_4). At −1.3 V, the reaction rate is very slow, thus it is feasible for us to monitor the reduction process of one kind of the electrochemically active groups on GO as function of electrochemical reduction time. As shown in Figure 3, when the electrochemical reduction time extends, the capacitance of the modified electrode decreases due to the increased electrical conductivity of ERGO, which results in the decrease of the reversible redox current peaks originating from the deoxidization of the oxygen functionalities.

In the following experiments, the electrochemical reduction of GO on graphite electrode was performed at controlled potentials. When the reduction potential was set at −0.8 V where the reduction current starts, partly reduced products were obtained. When the potential moved to −1.5 V, it results in the attachment of a bulk amount of black precipitate onto the bare graphite electrode due to the reduction of

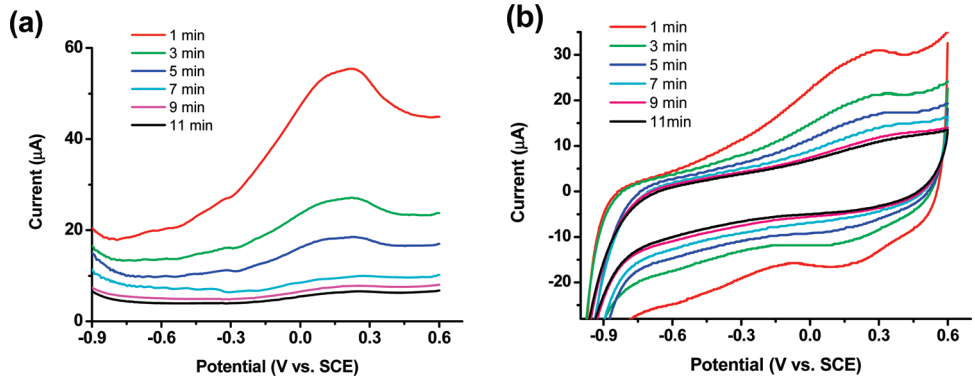

Figure 3. DPVs (a) and CVs (b) of the ERGO/GCE (electrochemically reduced at −1.3 V for different time) in 5 mM HCl at a scan rate of 100 mV s^{-1}.

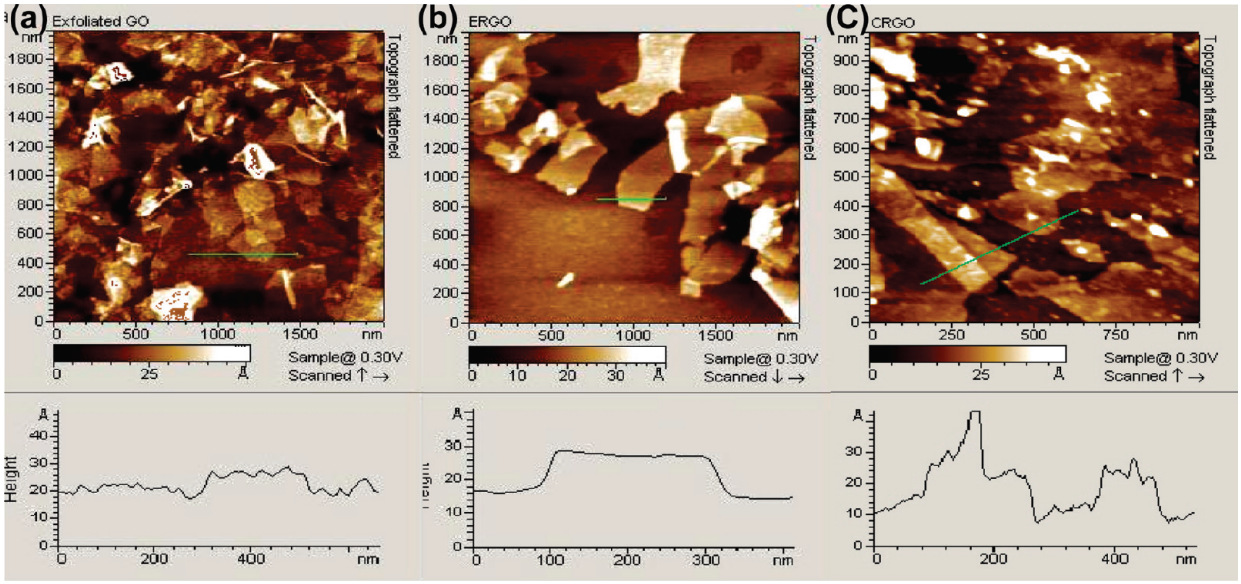

Figure 4. Tapping mode AFM images of the exfoliated GO (a), ERGO (b), and CRGO (c) with height profiles. The samples were prepared by drop-casting corresponding dilute dispersions onto mica sheets.

oxygenated GO. Further, the yellow color of the native GO suspension turns colorless. Meanwhile, hydrogen gas bubbles evolution from the reduction of water was also observed. It is found that more negative potentials require less time for the GO reduction. Magnetic stirring of the GO dispersion plays two important roles: propelling GO species onto the electrode surface and getting rid of gas bubbles to prevent the nanosheets falling off. The precipitates deposited at the potentials −1.5 and −1.3 V were subjected to characterizations.

Morphology Characterization. Atomic force microscopy (AFM) is currently the foremost methods allowing definitive identification of single-layer crystals.[9] Figure 4 shows the atomic force microscopy of the exfoliated GO, ERGO, and CRGO (chemically reduced GO). The graphite electrode attached with ERGO was first immersed into water several times for rinse (removal of GO or salts from the electrode surface). Then, the electrode was stirred in water softly to disperse loosely attached ERGO. A piece of mica immersed into the dispersion was employed for AFM characterization. As shown in Figure 4a, the exfoliated GO are flat sheets with an average thickness of about 1.1 nm. Thickness of the ERGO sheets is also about 1.1 nm and its lateral dimension is about 320 nm. The homogeneous atomic thickness might be due to the release of hydrogen. CRGO sheets are stacked in disorder on the mica substrate.

In Figure 5, the graphene nanosheets obtained by electrochemical reduction were analyzed by TEM and high magnification HRTEM observations. Large graphene nanosheets on the top of the carbon film were observed, and their resemblance of crumpled silk veil waves that were corrugated and scrolled are intrinsic to graphene nanosheets.[26] The graphene nanosheets are transparent and exhibit a very stable nature under the electron beam. From the HRTEM of image, the edges of the suspended film always fold back, allowing for a cross-section view of the film and the ordered graphitic lattices are clearly visible which can also be found in CRGO.[21,27,28] The graphitic laminar structure can be resolved in the ordered region as shown in the selected area electron diffraction (SAED) in the inset in Figure 5b. The well-defined diffraction spots confirm the crystalline structure of the graphene nanosheets obtained *via* electrochemical reduction of graphite oxide.

Spectroscopic Characterizations. Vacuum FT-IR spectroscopy was used to indicate the degree of removing the oxygen groups, and the IR absorption of water from the air is mainly eliminated. Figure 6 shows the vacuum FT-IR transmittance spectra (KBr) of pristine graphite (a), exfoliated GO (b), ERGO (c), and CRGO (d). The spectra are shifted downward for easy viewing. The spectrum of graphite oxide illustrates O−H (ν(carboxyl)) at ~1395 cm^{-1}, O−H (broad coupling ν(O−H)) at ~ 3200 cm^{-1} originated from carboxylic acid, while the band

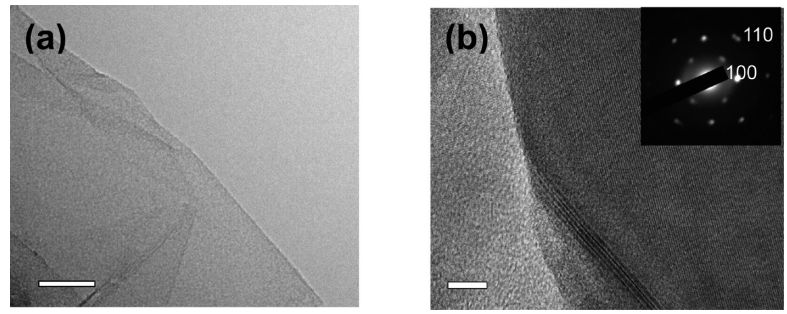

Figure 5. TEM (a) and HRTEM (b) images of the graphene nanosheets prepared by electrochemical reduction of the GO dispersion at −1.5 V. The inset in panel b is the selected area electron diffraction pattern (SAED). Scale bars: (a) 100 nm, and (b) 5 nm.

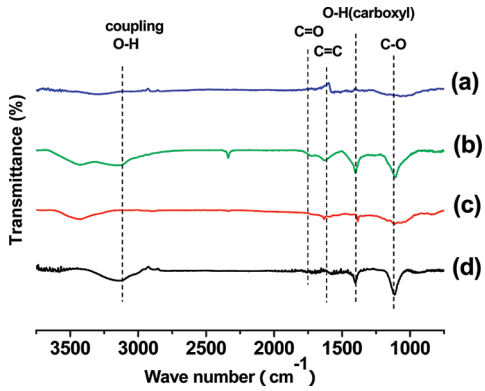

Figure 6. FTIR transmittance spectra of pristine graphite (a), exfoliated GO (b), ERGO (c), CRGO (d).

at *ca.* 3440 cm^{-1} could be due to the O−H stretching mode of intercalated water), C−O (ν(epoxy or alkoxy)) at ~1059 cm^{-1}, and C═O in carboxylic acid and carbonyl moieties (ν(carbonyl)) at 1740 cm^{-1}; C═C at ~1620 cm^{-1} assigns to skeletal vibrations of unoxidized graphitic domains or contribution from the stretching deformation vibration of intercalated water.[29,30] After the exfoliated GO is chemically reduced, the C═O vibration band disappears, the broad O−H and the C−O stretching bands remain. As the exfoliated GO is electrochemically reduced, the adsorption bands of oxygen functionalities disappear (carboxyl groups are considerably decreased, also found in pristine graphite) and only the peak at 1620 cm^{-1} remains, which is similar to that of pristine graphite, demonstrating high purity of graphene can be achieved by using the electrochemical approach.

At −1.3 V the reaction rate for electrochemical reduction of GO slows down, thus we can distinguish different product at its different reducing states, easily seen in cyclic voltammograms or differential pulse voltammetries. In the measured IR spectra (Figure 7) at −1.3 V, C═O group in products can be easily converted with the reduction time; however, functional

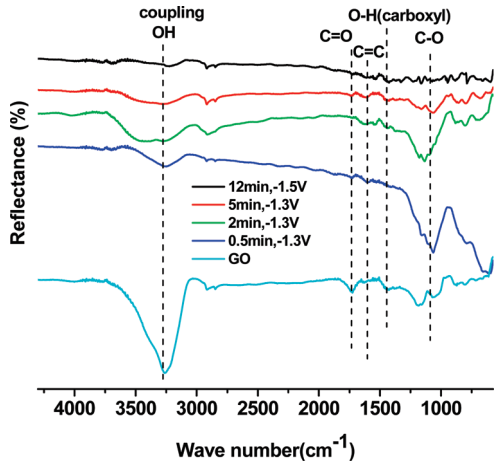

Figure 7. FTIR reflectance spectra of GO, ERGO at −1.3 V for different reduction time, and final product of ERGO at −1.5 V for 12 min.

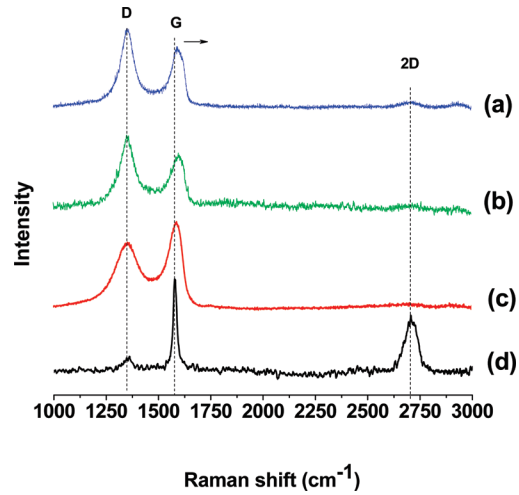

Figure 8. Raman spectra of ERGO (a), CRGO (b), exfoliated GO (c), and pristine graphite (d).

groups of O−H and C−O−C are very hard to be reduced. These functional groups of OH and C−O−C can only be reduced at more negative potentials (*i.e.*, −1.5 V). Since graphite disk as the working electrode was used in the electrochemical reduction, its weak absorption could also contribute to the resultant spectra. Therefore, the spectra are much more complicated than those transmittance ones obtained from KBr. Here, a MCT detector is used to increase the sensitivity.

Raman spectroscopy is a powerful nondestructive tool to distinguish ordered and disordered crystal structures of carbon. G band is usually assigned to the E_{2g} phonon of C sp^2 atoms, while D band is a breathing mode of κ-point phonons of A_{1g} symmetry.[31] Figure 8 shows the Raman spectra of ERGO (a), CRGO (b), exfoliated GO (c), and pristine graphite (d) samples. Raman spectrum of the pristine graphite displays a strong G band at 1579 cm^{-1}, a weak D band at 1360 cm^{-1}, and a middle 2D band at 2700 cm^{-1}. In the Raman spectra of the exfoliated GO, CRGO, and ERGO, the G band is broadened and shifted upward to 1595 cm^{-1}, which was mainly caused by stress.[32] At the same time, intensity of the D band at 1360 cm^{-1} of exfoliated GO increases substantially, indicating the decrease in size of the in-plane sp^2 domains, possibly due to the extensive oxidation and ultrasonic exfoliation.[19] When the exfoliated GO is electrochemically or chemically reduced, the intensity of the D band increases further. This can be due to defects introduced into the ERGO and CRGO during prepration.[32,33] In addition, there is a significant change in 2D band of ERGO compared to bulk graphite. The weak and broadened 2D peak shows that ERGO possesses some defects because of the fast reduction rate; these local defects can hardly recover in time. These defects could be further eliminated by performing the electrochemical reduction at elevated temperature or annealing the products. However, an increased D/G intensity ratio of ERGO compared to that of the exfoliated GO is observed. This change suggests a de-

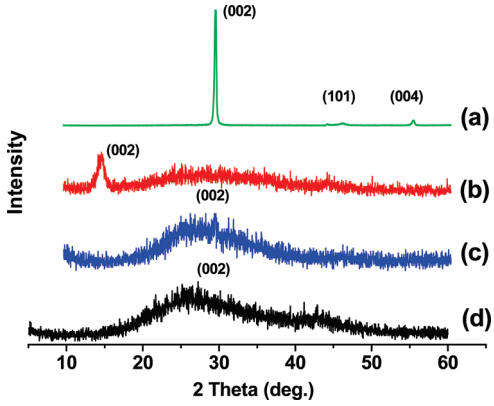

Figure 9. X-ray diffraction patterns of the pristine graphite (a), exfoliated GO (b), ERGO (c) and CRGO (d).

crease in the average size of the sp^2 domains upon reduction of the exfoliated GO[19] and can be explained by the creation of numerous new graphitic domains that are smaller in size than the ones presented in exfoliated GO.

XRD Characterization. XRD patterns of the pristine graphite, exfoliated GO, CRGO, and ERGO are recorded in Figure 9. Compared with the pristine graphite, the feature diffraction peak of exfoliated GO appears at 10.4° (002) as the AB stacking order is still observed in graphite oxide with layer-to-layer distance (*d*-spacing) of 0.849 nm.[30] This value is larger than the *d*-spacing (0.335 nm) of pristine graphite (2 theta. = 26.6°) due to the intercalated water molecules between layers.[29,34] After the exfoliated GO is electrochemically reduced, the diffraction peak of ERGO is at 26.6° (similar to the result of CRGO).

Electrical Conductivity of Graphene Sheets. The electrical conductivity is perhaps the best indicator of the extent to which graphite oxide has been reduced to graphene.[35] The electrical conductivity of the graphite oxide sheets and graphene nanosheets have been measured by the four-probe van der Pauw method which is often used to measure the Hall Effect.[36] The sheet resistivity (ρ) in Ohm meter of the sample can be calculated by

$$\rho = \frac{\pi d}{\ln 2}\frac{R_{12,34} + R_{23,41}}{2}f \qquad (1)$$

where *d* is thickness of a thin film, $R_{12,34}$ and $R_{23,41}$ are two resistances measured when each of adjacent current and voltage contacts are switched, and *f* is a correction factor based on the ratio of $R_{12,34}$ and $R_{23,41}$. The electrical conductivity of the pristine graphite, graphite oxide, and graphene nanosheets obtained by electrochemical and chemical routes are calculated to be ~9.0 × 10^4, ~2.0, ~3.5 × 10^3, and ~3.2 × 10^3 S/m, respectively (higher than previous reference reports).[27,37] This indicates that graphite oxide was reduced to graphene *via* both electrochemical and chemical process.

Electrocatalysis of Dopamine on Graphene-Modified Electrode. In electrochemical impedance spectra, the semicircle portion observed at high frequencies corresponds to the charge transfer limiting process. The charge transfer resistance R_t can be directly measured as the semicircle diameter. As we can see from Figure 10a, when exfoliated GO is modified onto a GCE surface, the semicircle dramatically increases as compared to the bare GCE, suggesting that the exfoliated GO acts as an insulating layer which makes the interfacial charge transfer difficult and the surface charges of the exfoliated GO repel the access of ferricyanide and ferrocyanide ions to the electrode surface for electron communication as well. After the exfoliated GO film is electrochemically reduced on the electrode at −1.5 V, the semicircles decrease distinctively, indicating that ERGO has accelerated electron transfer between the electrochemical probe $[Fe(CN)_6]^{3-/4-}$ and the electrode, and the main reason is attributed to significantly improved electrical conductivity of the ERGO films, presumably owing to the restoration of a graphitic network of sp^2 bonds.[5] Besides, we find that ERGO shows good electrocatalytic activity toward dopamine (DA). In Figure 10b, it is inter-

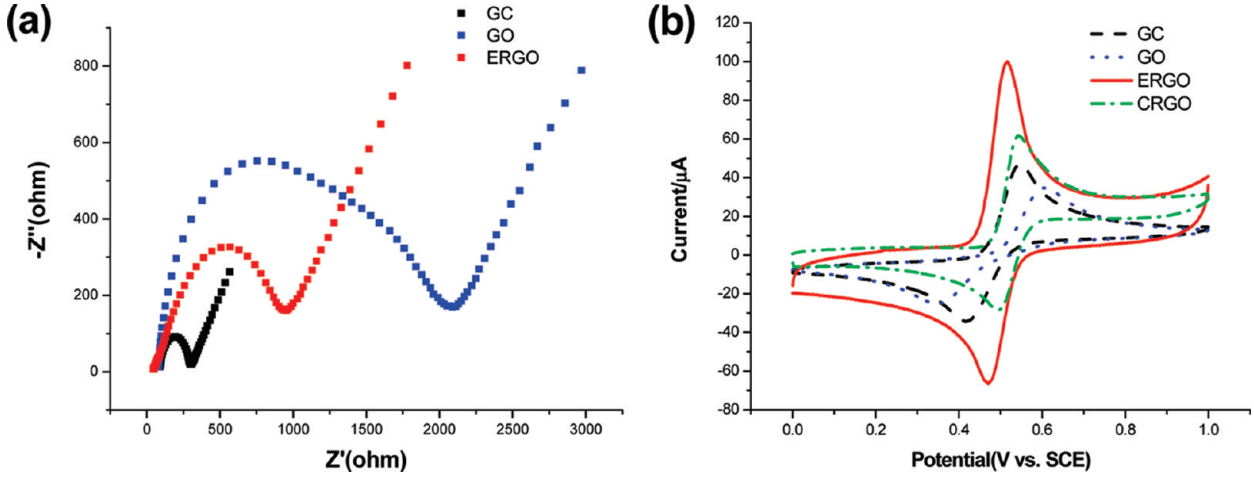

Figure 10. Nyquist diagrams and cyclic voltammograms obtained at a bare glass carbon electrode, exfoliated GO/GCE, CRGO/GCE, and ERGO/GCE. (a) 10.0 mM $Fe(CN)_6^{3-}/Fe(CN)_6^{4-}$ (1:1) mixture with 0.1 M KCl, (b) 1 mM DA in 0.1 M H_2SO_4, scan rate: 200 mV s^{-1}.

esting to observe a quite reversible redox couple for DA. The peak separation potential is only $\Delta E_p = 44$ mV (solid curve) which is much lower than that of DA/CRGO ($\Delta E_p \approx 51$ mV, dash-dotted curve) as well as the previous reported one at mesoporous carbon or graphene (chemically reduced from GO)-modified glass carbon electrode.[38,39] In addition, a larger peak current of dopamine on the graphene-modified electrode appears as compared to the GO/GCE (dotted curve). This electrocatalytic activity toward dopamine could be due to the unique electronic properties of graphene which accelerates electron transfer rate *via* improved conductivity and the good affinity of graphene to dopamine. Although the real electrocatalytic mechanism of dopamine on graphene-modified electrode is not yet clear (which is undergoing in our laboratory).

CONCLUSION

In summary, a green and fast electrochemical approach to the synthesis of graphene nanosheets is reported using exfoliated graphite oxide (GO) as precursor. This method is green and will not result in contamination of the product graphene. However, the electrochemical-reduced graphene possesses some defects due to the fast reduction rate. These defects could be eliminated by performing the electrochemical reduction at elevated temperature or annealing the products, which are undergoing in our lab. The present method can be used to prepare graphene nanosheets in large scale and graphene sheets modified electrodes used for further application in electrocatalysis and biosensors which are undergoing in the laboratory.

EXPERIMENTAL SECTION

Materials and Methods. Graphite oxide (GO) was synthesized from spectral graphite (about 50 μm, Shanghai Carbon Co., Ltd.) by the modified Hummers method as originally presented by Kovtyukhova and colleagues.[24,25] The as-synthesized GO was suspended in water to give a brown dispersion, which was subjected to dialysis for one week to completely remove residual salts and acids. Exfoliated graphite oxide (exfoliated GO) was obtained by ultrasound of the 0.5 wt % GO dispersion, using a Sonifier (KQ 100E, 100 W, Kunshan, China). The obtained brown dispersion was then subjected to 5 min of centrifugation at 3000 rpm to remove any unexfoliated graphite oxide (an extremely small amount) using an Allegra 64R centrifuge (Beckman Coulter with a rotor of F1010). All the aqueous solutions were prepared with Millipore water having a resistivity of 18.2 MΩ (Purelab Classic Corp., USA).

Chemical reduced graphite oxide (CRGO) was prepared using ammonia and hydrazine hydrate as reducing agents according to references 19 and 21 to compare it with the present electrochemically reduced graphite oxide (ERGO) in all characterizations. The electrochemical reduction of GO suspension in large scale on the working electrode of graphite was carried out in a three-electrode system (Pt as counter electrode, saturated calomel electrode as reference electrode) with CHI 630a Electrochemical Workstation (CH Instruments, USA) as the power supply stirring for 2 h. Glassy carbon electrode (GCE) was polished with alumina powders, then rinsed thoroughly, and finally dried with blowing N_2. A 5 μL portion of exfoliated GO suspension was spread on a pretreated bare GCE or on graphite disk using a micropipet tip. The film was dried in a vacuum desiccator. The electrochemical reduction of the pretreated exfoliated GO film on GCE used in impedance characterization and electrocatalysis study of dopamine and the pretreated exfoliated GO film on graphite discs used in reflection IR was performed on a CHI at a constant potential (−1.5 or −1.3 V *vs* SCE) in 10 mmol/L pH 5.0 PBS (K_2HPO_4/KH_2PO_4). Electrochemical impedance spectroscopy (EIS) experiments were conducted with an Autolab Electrochemical Analyzer (Ecochemie, Netherlands). All experiments were carried out at room temperature.

Characterization. Atomic force microscope (AFM) images were acquired by using an Agilent 5500 AFM/SPM system with Picoscan v5.3.3 software. All the images presented in this article were acquired using tapping mode under ambient conditions. FT-IR spectra were recorded on a Bruker (Germany) VERTEX 80v vacuum FT-IR spectrometer over a range from 400 to 4500 cm^{-1} with DTGS or MCT as detector. Raman scattering was performed on a JY-HR800 Raman spectrometer using a 488-nm laser source. X-ray diffraction (XRD) was performed with a XRD-6000 X-ray diffractometer (Shimadzu, Japan) using Cu Kα radiation. High resolution transmission electron microscopy (TEM) was obtained on JEM-2100 (Japan), and the accelerating voltage was 200 kV.

Acknowledgment. This work was financially supported by the National Basic Research Program (2007CB714501), the National Natural Science Foundation of China (NSFC: 20535010, 20775035, 20828006, 20821063), and Natural Science Foundation of Jiangsu Province (BK2007147).

REFERENCES AND NOTES

1. Katsnelson, M. I. Graphene: Carbon in Two Dimensions. *Mater. Today* **2007**, *10*, 20–27.
2. Avouris, P.; Chen, Z.; Perebeinos, V. Carbon-Based Electronics. *Nat. Nanotechnol.* **2007**, *2*, 605–615.
3. Son, Y. W.; Cohen, M. L.; Louie, S. G. Half-Metallic Graphene Nanoribbons. *Nature* **2006**, *444*, 347–349.
4. Schedin, F.; Geim, A. K.; Morozov, S. V.; Hill, E. M.; Blake, P.; Katsnelson, M. I.; NovoselovK, S. Detection of Individual Gas Molecules Adsorbed on Graphene. *Nat. Mater.* **2007**, *6*, 652–655.
5. Sakhaee-Pour, A.; Ahmadian, M. T.; Vafai, A. Potential Application of Single-Layered Graphene Sheets as Strain Sensor. *Solid State Commun.* **2008**, *147*, 336–340.
6. Stankovich, S.; Dikin, D. A.; Dommett, G. H. B.; Kohlhaas, K. M.; Zimney, E. J.; Stach, E. A.; Pinen, R. D.; Nguyen, S. T.; Ruoff, R. S. Graphene-Based Composite Materials. *Nature* **2006**, *442*, 282–286.
7. Watcharotone, S.; Dikin, D. A.; Stankovich, S.; Piner, R.; Jung, I.; Mommett, G. H. B.; Evmenenko, G.; Wu, S. E.; Chen, S. F.; Liu, C. P.; *et al.* Graphene-Silica Composite Thin Films as Transparent Conductors. *Nano Lett.* **2007**, *7*, 1888–1892.
8. Takamura, T.; Endo, K.; Fu, L.; Wu, Y. P.; Lee, K. J.; Matsumoto, T. Identification of Nano-Sized Holes by TEM in the Graphene Layer of Graphite and the High Rate Discharge Capability of Li-Ion Battery Anodes. *Eletrochim. Acta* **2007**, *53*, 1055–1061.
9. Novoselov, K. S.; Jiang, D.; Schedin, F.; Booth, T. J.; Khotkevich, V. V.; Morozov, S. V.; Geim, A. K. Two-Dimensional Atomic Crystals. *Proc. Natl. Acad. Sci. U.S.A.* **2005**, *102*, 10451–10453.
10. Geim, A. K.; Novoselov, K. S. The Rise of Graphene. *Nat. Mater.* **2007**, *6*, 183–191.
11. Novoselov, K. S.; Geim, A. K.; Morozov, S. V.; Jiang, D.; Zhang, Y.; Dubonos, S. V.; Grigorieva, I. V.; Firsov, A. A. Electric Field Effect in Atomically Thin Carbon Films. *Science* **2004**, *306*, 666–669.
12. Charrier, A.; Coati, A.; Argunova, T.; Garreau, Y.; Pinchaux, R.; Forbeaux, I.; Debever, J. M.; Sauvage-Simkin, M.;

Themlin, J. M. Solid-State Decomposition of Silicon Carbide for Growing Ultra-thin Heteroepitaxial Graphite Films. *J. Appl. Phys.* **2002**, *92*, 2479–2484.
13. Berger, C.; Song, Z. M.; Li, T. B.; Li, X. B.; Ogbazghi, A. Y.; Feng, R.; Dai, Z. T.; Marchenkov, A. N.; Conrad, E. H.; First, P. N.; de Heer, W. Ultrathin Epitaxial Graphite: 2D Electron Gas Properties and a Route Toward Graphene-Based Nanoelectronics. *J. Phys. Chem. B* **2004**, *108*, 19912–19916.
14. Berger, C.; Song, Z. M.; Li, X. B.; Wu, X. S.; Brown, N.; Naud, C.; Mayou, D.; Li, T. B.; Hass, J.; Marchenko, A. N.; *et al.* Electronic Confinement and Coherence in Patterned Epitaxial Graphene. *Science* **2006**, *312*, 1191–1196.
15. Chen, G. H.; Wenig, W. G.; Wu, D.; Wu, C. L. PMMA/Graphite Nanosheets Composite and Its Conducting Properties. *Eur. Polym. J.* **2003**, *39*, 2329–2335.
16. Chen, G. H.; Wenig, W. G.; Wu, D.; Wu, C. L. Preparation of Polystyrene/Graphite Nanosheet Composite. *Polymer* **2003**, *44*, 1781–1784.
17. Chen, G. H.; Wenig, W. G.; Wu, D. J.; Wu, C. L.; Lu, J. R.; Wang, P. P.; Chen, X. F. Preparation and Characterization of Graphite Nanosheets from Ultrasonic Powdering Technique. *Carbon* **2004**, *42*, 753–759.
18. Stankovich, S.; Piner, R. D.; Chen, X. Q.; Wu, N. Q.; Nguyen, S. T.; Ruoff, R. S. Stable Aqueous Dispersions of Graphitic Nanoplatelets *via* the Reduction of Exfoliated Graphite Oxide in the Presence of Poly(sodium 4-styrenesulfonate). *J. Mater. Chem.* **2006**, *16*, 155–158.
19. Stankovich, S.; Dikin, D. A.; Piner, R. D.; Kohlhaas, K. A.; Kleinhammes, A.; Jia, Y. Y.; Wu, Y.; Nguyen, S. T.; Ruoff, R. S. Synthesis of Graphene-Based Nanosheets *via* Chemical Reduction of Exfoliated Graphite Oxide. *Carbon* **2007**, *45*, 1558–1565.
20. Li, D.; Muller, M. B.; Gilje, S.; Kaner, R. B.; Wallace, G. G. Processable Aqueous Dispersions of Graphene Nanosheets. *Nat. Nanotechnol.* **2008**, *3*, 101–105.
21. Wang, G. X.; Yang, J.; Park, J.; Gou, X. L.; Wang, B.; Liu, H.; Yao, J. Facile Synthesis and Characterization of Graphene Nanosheets. *J. Phys. Chem. C* **2008**, *112*, 8192–8195.
22. Williams, G.; Seger, B.; Kamat, P. V. TiO_2-Graphene Nanocomposites UV-Assisted Photocatalytic Reduction of Graphene Oxide. *ACS Nano* **2008**, *2*, 1487–1491.
23. Hernandez, Y.; Nicolosi, V.; Lotya, M.; Blighe, F. M.; Sun, Z. Y.; De, S.; McGovern, I. T.; Holland, B.; Byrne, M.; Gunko, Y; *et al.* High-Yield Production of Graphene by Liquid-Phase Exfoliation of Graphite. *Nat. Nanotechnol.* **2008**, *3*, 563–568.
24. Kovtyukhova, N. I.; Ollivier, P. J.; Martin, B. R.; Mallouk, T. E.; Chizhik, S. A.; Buzaneva, E. V.; Gorchinskiy, A. D. Layer-by-Layer Assembly of Ultrathin Composite Films from Micron-Sized Graphite Oxide Sheets and Polycations. *Chem. Mater.* **1999**, *11*, 771–778.
25. Hummers, W. S.; Offeman, R. E. Preparation of Graphitic Oxide. *J. Am. Chem. Soc.* **1958**, *80*, 1339.
26. Meyer, J. C.; Geim, A. K.; Katsnelson, M. I.; Novoselov, K. S.; Booth, T. J.; Roth, S. The Structure of Suspended Graphene Sheets. *Nature* **2007**, *446*, 60–63.
27. Reina, A.; Jia, X. T.; Ho, J.; Nezich, D.; Son, H.; Bulovic, V.; Dresselhaus, M. S.; Kong, J. Large Area, Few-Layer Graphene Films on Arbitrary Substrates by Chemical Vapor Deposition. *Nano Lett.* **2009**, *9*, 30–35.
28. Alwarappan, S.; Erdem, A.; Liu, C.; Li, C. Z. Probing the Electrochemical Properties of Graphene Nanosheets for Biosensing Applications. *J. Phys. Chem. C* **2009**, *113*, 8853–8857.
29. Hontoria-Lucas, C.; Lopez-Peinado, A. J.; Lopez-Gonzalez, J. D.; Rojas-Cervantes, M. J.; Martin-Aranda, R. M. Study of Oxygen-Containing Groups in a Series of Graphite Oxides: Physical and Chemical Characterization. *Carbon* **1995**, *33*, 1585–1592.
30. Jeong, H. K.; Lee, Y. P.; Lahaye, R. J.; Park, M. H.; An, K. H.; Kim, I. J.; Yang, C. W.; Park, C. Y.; Ruoff, R. S.; Lee, Y. H. Evidence of Graphitic AB Stacking Order of Graphite Oxides. *J. Am. Chem. Soc.* **2008**, *130*, 1362–1366.
31. Tuinstra, F.; Koenig, J. L. Raman Spectrum of Graphite. *J. Chem. Phys.* **1970**, *53*, 1126–1130.
32. Ni, Z. H.; Wang, H. M.; Ma, Y.; Kasim, J.; Wu, Y. H.; Shen, Z. X. Tunable Stress and Controlled Thickness Modification in Graphene by Annealing. *ACS Nano* **2008**, *2*, 1033–1039.
33. Gupta, A.; Chen, G.; Joshi, P.; Tadigadapa, S.; Eklund, P. C. Raman Scattering from High-Frequency Phonons in Supported *n*-Graphene Layer Films. *Nano Lett.* **2006**, *6*, 2667–2673.
34. Buchsteiner, A.; Lerf, A.; Pieper, J. Water Dynamics in Graphite Oxide Investigated with Neutron Scattering. *J. Phys. Chem. B* **2006**, *110*, 22328–22338.
35. Si, Y. C.; Samulski, E. T. Synthesis of Water Soluble Graphene. *Nano Lett.* **2008**, *8*, 1679–1682.
36. van der Pauw, L. J. A Method of Measuring Specific Resistivity and Hall Effect of Discs of Arbitrary Shape. *Philips Res. Rep.* **1958**, *13*, 1–9.
37. Choucair, M.; Thordarson, P.; Stride, J. A. Gram-Scale Production of Graphene Based on Solvothermal Synthesis and Sonication. *Nat. Nanotechnol.* **2009**, *4*, 30–33.
38. Jia, N. Q.; Wang, Z. Y.; Yang, G. F.; Shen, H. B.; Zhu, L. Z. Electrochemical Properties of Ordered Mesoporous Carbon and Its Electroanalytical Application for Selective Determination of Dopamine. *Electrochem. Commun.* **2006**, *9*, 233–238.
39. Wang, Y.; Li, Y. M.; Tang, L. H.; Lu, J.; Li, J. H. Application of Graphene-Modified Electrode for Selective Detection of Dopamine. *Electrochem. Commun.* **2009**, *11*, 889–892.